

# Features of the Temperature Distribution in Flat Conductors with Different Configurations

T. N. Gerasimenko<sup>a</sup> and P. A. Polyakov<sup>b, \*</sup>

<sup>a</sup>OOO NTTs Bioklinikum, Moscow, 115088 Russia

<sup>b</sup>Faculty of Physics, Moscow State University, Moscow, 119991 Russia

\*e-mail: polyakovpa@mail.ru

**Abstract**—Steady-state temperature distributions in flat conductors of different configurations with direct electric current flowing inside them are investigated. It is shown that the temperature distributions are determined not only by the properties of a material, but also by the characteristic dimensions of a conductor and do not necessarily correlate with the current distributions. Criteria for the similarity between temperature distributions in geometrically identical flat conductors are established.

DOI: 10.3103/S1062873818020119

## INTRODUCTION

Studying the distribution of current in a flat conductor with thickness  $\tau$  much smaller than its linear size often yields a solution that contains a singularity in one or several points of the conductor [1–4]. This singularity can be eliminated by correcting model errors [5], but it is obvious that a conductor of complex configuration can contain regions where the current density will be much higher than in the rest of the conductor.

According to the Joule–Lenz law, the maximum amount of heat is obviously released in these regions, so it is natural to assume that the conductor is heated most in them. To qualitatively understand features of the temperature distribution in such a situation, we analytically investigated the case of a singularity in the current distribution in a problem with cylindrical symmetry [6]. It was found that, although bulk heat conduction greatly smooths the nonuniformity of heat release, thus making the temperature distribution different from the distribution of the released heat power, the temperature maximum coincides with that of the current density.

To study the temperature distributions when there is no symmetry, we investigated several conductors bent at different angles, and a conductor with a rectangular cut. Figure 1 presents the current density distributions in these conductors [4, 5], which show that the current density grows sharply near their corners. Unfortunately, the heat-conduction equation cannot be solved analytically for such conductors, and requires the use of numerical methods.

## HEAT-CONDUCTION EQUATION IN DIMENSIONLESS VARIABLES

In solving the temperature distribution problem, we considered that a heat distribution is affected by both the bulk thermal conductivity and the heat release from a conductor's surface. The latter was described using the Newton–Richmann law with the effective heat-transfer coefficient in [7–9], which was considered constant.

It was noted that in most metals, the temperature dependence of the resistivity is described by a linear function in a wide range of temperatures [10, 11]:

$$\rho = \rho_0 (1 + \alpha(T - \theta)),$$

where  $\alpha$  is the temperature resistance coefficient;  $\theta$  is the environmental temperature, which was assumed to be constant;  $\rho_0$  is the resistivity of a conductor material at this temperature; and  $T$  is the desired conductor temperature.

In light of these assumptions, the heat-conduction equation can be written as [6]

$$\tau\beta\Delta u - h_T u = -\tau j^2 \rho_0 (1 + \alpha u), \quad (1)$$

where  $u(x, y) = T(x, y) - \theta$ ;  $\beta$  is the thermal conductivity coefficient;  $h_T$  is the effective heat-transfer coefficient; and  $\tau$  is the conductor's thickness.

Since the current distributions in geometrically identical conductors are also the same, the distributions of the released heat energy will be similar when the current densities of the investigated conductors coincide. However, the redistribution of this energy over a conductor is governed by the bulk thermal con-

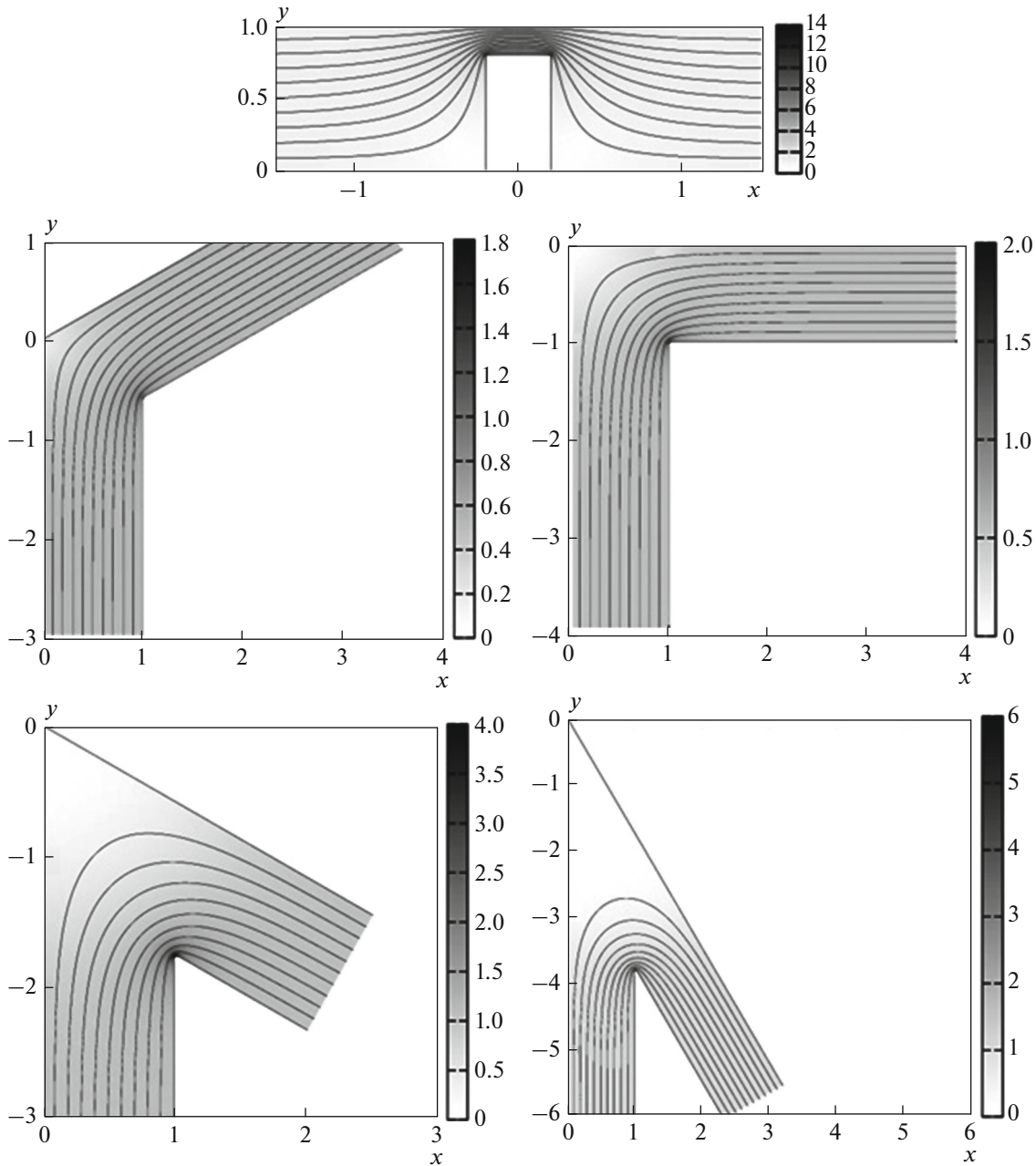


**Fig. 1.** Normalized current density distributions  $j(x, y)/j_\infty$  and current lines in the investigated conductors [4, 5];  $j_\infty$  is the current density in the region infinitely remote from the inhomogeneity.

ductivity, which is described by the Fourier law. In other words, it depends on the temperature gradient and thus the characteristic sizes of the conductor.

To investigate the similarity between temperature distributions, Eq. (1) was written in dimensionless variables. According to the Buckingham  $\Pi$  theorem [12], the number of these can be reduced to three:

$$\Delta_{\Pi} \tilde{u} - (\Pi_1 - \Pi_\alpha \Pi_2) \tilde{u} = -\Pi_2, \quad (2)$$

where

$$\Pi_1 = L^2 \frac{h_T}{\beta \tau}, \quad \Pi_2 = \frac{L^2 \rho_0 j^2}{T \beta}, \quad \Pi_\alpha = T \alpha, \quad (3)$$

Here,  $L$  and  $T$  are the characteristic length and temperature, respectively;  $\Delta_{\Pi}$  is the Laplacian in dimensionless coordinates;  $\tilde{x} = x/L$ ;  $\tilde{y} = y/L$ ; and  $\tilde{u} = u/T$ .

As expected, it follows from expressions (3) that the shape of temperature distributions is affected by the

characteristic sizes of the conductors. It can be seen that parameter  $\Pi_1$  is proportional to the squared characteristic size of a conductor, but does not depend on the current flowing through it. This indicates that a change in characteristic sizes of a conductor alters the form of Eq. (2) and thus its solution.

In solving Eq. (2), we assumed the conductors to be surrounded by a fully heat-insulating material from their side walls and the outflow of heat through the side walls to be zero. To use numerical methods, we considered finite regions of a conductor and set their boundaries in places where the current lines can be considered uniform. Since the current and thus the heat sources were uniformly distributed, we assumed the temperature gradient to be negligible, i.e., Neuman conditions

$$\begin{cases} \Delta_{\Pi} \tilde{u} - [\Pi_1 - \Pi_{\alpha} \Pi_2(\tilde{x}, \tilde{y})] \tilde{u} = -\Pi_2(\tilde{x}, \tilde{y}) \\ \text{when } (\tilde{x}, \tilde{y}) \in \Omega, \\ \frac{\partial \tilde{u}}{\partial \tilde{n}} = 0 \text{ when } (\tilde{x}, \tilde{y}) \in \partial\Omega, \end{cases} \quad (4)$$

to be specified over the entire boundary of the investigated region of the conductor. Here,  $\Omega$  is the investigated region of the conductor in dimensionless coordinates. According to [13], this was equivalent to the functional minimization problem

$$\begin{aligned} & \chi[\tilde{u}, \partial_{\tilde{x}} \tilde{u}, \partial_{\tilde{y}} \tilde{u}] \\ & = \int_{\Omega} \left( \frac{1}{2} [(\partial_{\tilde{x}} \tilde{u})^2 + (\partial_{\tilde{y}} \tilde{u})^2] \right. \\ & \left. + (\Pi_1 - \Pi_{\alpha} \Pi_2) \tilde{u}^2 \right) - \Pi_2 \tilde{u} \Big) dS, \end{aligned} \quad (5)$$

which allowed us to solve it using the finite-element method.

To use the latter, we considered all the investigated regions to be obtained from the upper complex semi-plane using conformal mapping [4, 5]. This allowed us to choose triangulation points not inside the  $\Omega$  region, but in the corresponding semi-ring of the upper complex semi-plane. This in turn enabled us to avoid difficulties in selecting points at the boundary and to use the same algorithm for all investigated regions.

A Delaunay triangulation was built using the TRIANGLE program [14] and the resulting system of linear equations was solved using the UMFPAK library [15].

The solutions for aluminum conductors with thickness  $\tau = 10 \mu\text{m}$  and a current flowing with a density of  $j_{\infty} = 50 \text{ A mm}^{-2}$  are presented in Fig. 2. The ambient temperature was  $\theta = 26.6^{\circ}\text{C}$ , and the parameters of the material were  $\rho = 0.0292 \Omega \text{ mm}^2 \text{ m}^{-1}$ ;  $\beta = 226 \text{ W K}^{-1} \text{ m}^{-1}$ ;  $h_T = 49.6 \text{ W K}^{-1} \text{ m}^{-2}$ ; and  $\alpha = 0.0042 \text{ K}^{-1}$ . It can be

seen that upon variation in characteristic size  $L$ , the temperature distributions change strongly and the temperature at the point with the maximum current density can be either higher or lower than that of parts of the conductor far from an inhomogeneity. In addition, the temperature spread in conductors with smaller characteristic sizes is much smaller, so conductors can appear to be uniformly heated when there is insufficient accuracy of measurement.

## EXPERIMENTAL

Temperature distributions were studied experimentally using a SAT-S160 infrared thermograph that provided both temperature distribution patterns and temperatures at separate conductor points. The achievable temperature measurement error was  $2^{\circ}\text{C}$ , and the spatial resolution was  $2.2 \text{ mrad}$ .

The measured samples were a 1-cm-wide conductor bent at an angle of  $90^{\circ}$  and a conductor of the same width with a rectangular gash where the extent of narrowing was 2 mm. The conductors were made of 10- $\mu\text{m}$ -thick aluminum foil with surfaces containing traces of technological processing. According to the calculations made at different radii of curvature, the temperature of the interior angle in such conductors is equal to or slightly exceeds the ones far from the bend. In addition, we measured the temperatures of two conductors in the form of strips 1.1 and 2 mm wide.

To bring the spectral characteristics of the conductors' heat radiation closer to those of a black body, the conductors were coated with paint based on carbon black.

The conductors were heated by a direct electric current induced by a standard Mastech DC HY3030E power source that generated currents of up to 30 A. The integral current flowing through each conductor was detected by a built-in digital device with an error of up to 0.1 A. The maximum current through the sample was limited by a constantan rheostat.

The heat-transfer coefficient was obtained empirically by assuming that in the stationary mode, the temperature of a straight conductor without bends is determined as

$$u = \frac{\rho_{\theta} j^2 \tau}{h_T - \alpha \rho_{\theta} j^2 \tau}. \quad (6)$$

Knowing the conductor temperature, we can find the heat-transfer coefficient:

$$h_T = \frac{\rho_{\theta} j^2 \tau (1 + \alpha u)}{u}. \quad (7)$$

This coefficient calculated for a 1.1-cm-wide strip was found to be  $49 \pm 5.5 \text{ W K}^{-1} \text{ m}^{-2}$ , which is qualitatively

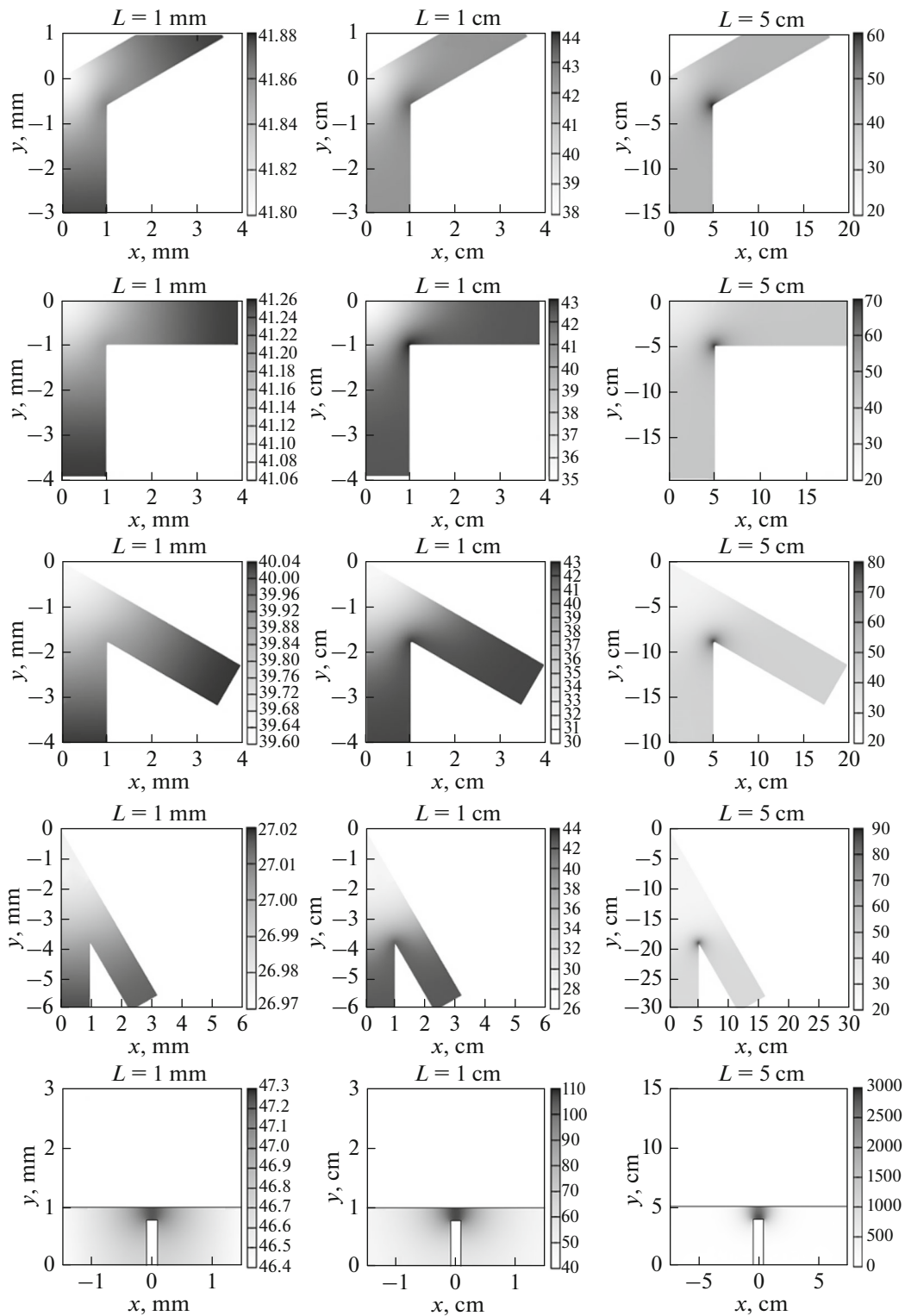


Fig. 2. Temperature distributions in geometrically similar conductors of different configurations.

consistent with the heat-transfer coefficient for a conductor with natural convection from above and below [1]. This value, which is somewhat higher than the one calculated, is explained by the investigated conductor

not being an absolutely black body. The measured temperature can appear lower than the real temperature, resulting in high heat-transfer coefficients in the calculations.

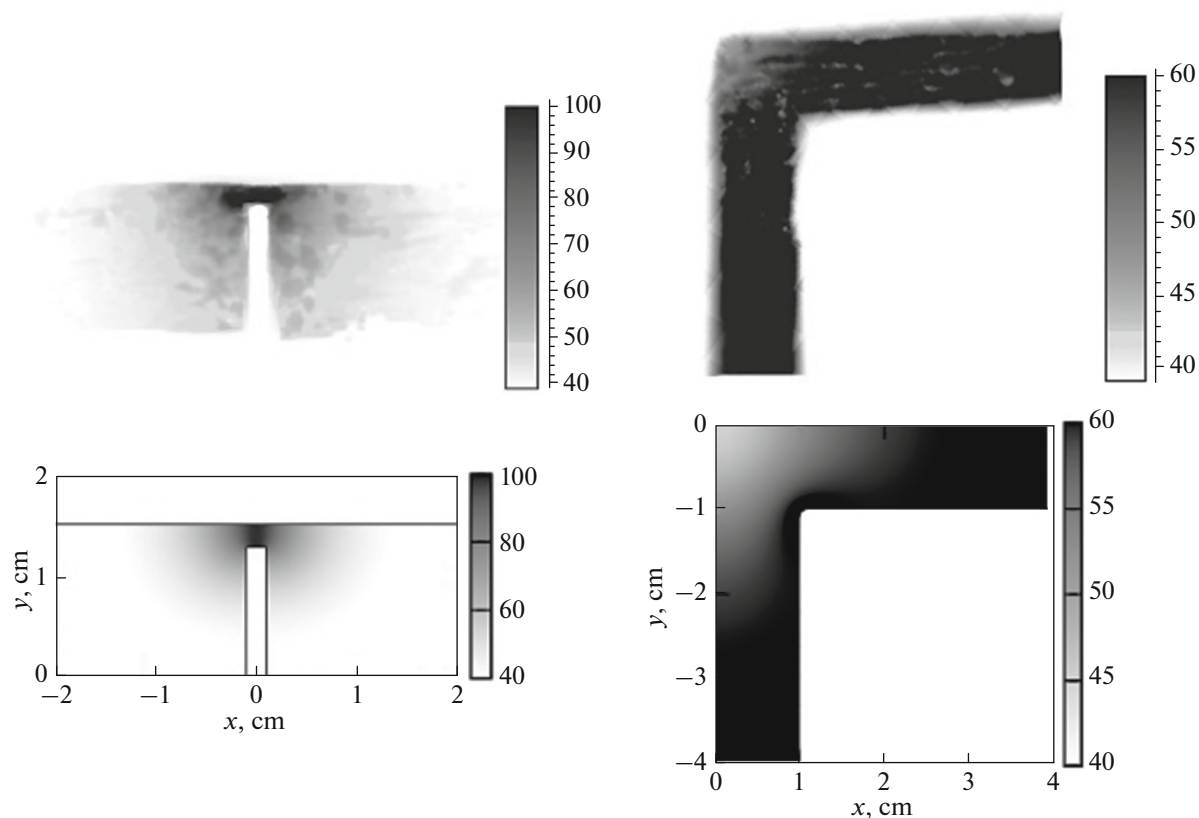


Fig. 3. Heat patterns and numerical calculation.

Figure 3 shows examples of heat patterns obtained using an IR thermograph and the corresponding numerical calculation data. For the conductor with a gash, the current is 5 A; for the conductor bent at the right angle, it is 7.1 A. Figure 4 shows experimental and theoretical flowing current dependences of the temperature near the interior angle of the conductor bent at a right angle and at the bypass center. The relatively wide temperature spread in the interior angle is related to the difficulty of focusing the device on the interior angle of the conductor, so the temperature was actually measured at some distance (about a millimeter) from it. This problem did not arise upon varying the bypass temperature, since the device had the option of searching for the maximum temperature corresponding to the bypass center.

Experimental verification was performed mainly because of a contradiction between the obtained theoretical data. It was aimed at qualitative testing of the temperature distributions, rather than achieving metrological accuracy. At the same time, we observed both qualitative and quantitative (within 30%) coincidence between the theory and experiment.

Measurements of the temperature of a 2-mm-thick defect-free strip showed that it was heated to a tem-

perature of around  $100^{\circ}\text{C}$  by currents of 2.9–3 A. Transferring heat to the wide part of a conductor allowed us to transmit twice the current through a bypass of the same width without breaking the bypass.

## CONCLUSIONS

Our investigations showed that the steady-state temperature distributions in flat conductors are determined not only by the characteristics of a conductor's material, but by a conductor's characteristic sizes as well. It was established that the role of bulk thermal conductivity grows considerably upon a reduction in the characteristic conductor sizes, resulting in strong redistribution of the temperature over a conductor. As a result, the temperatures of the regions of the maximum heat power release can be even lower than those of the regions where virtually no heat power is released. This leads in particular to a situation where, despite the presence of local defects that cause a sharp rise in current density in a conductor (e.g., in a conductor with a bypass), the conductors will not explode if their characteristic sizes are small.

The obtained similarity criteria allow us to choose the materials and conditions for cooling conductors to

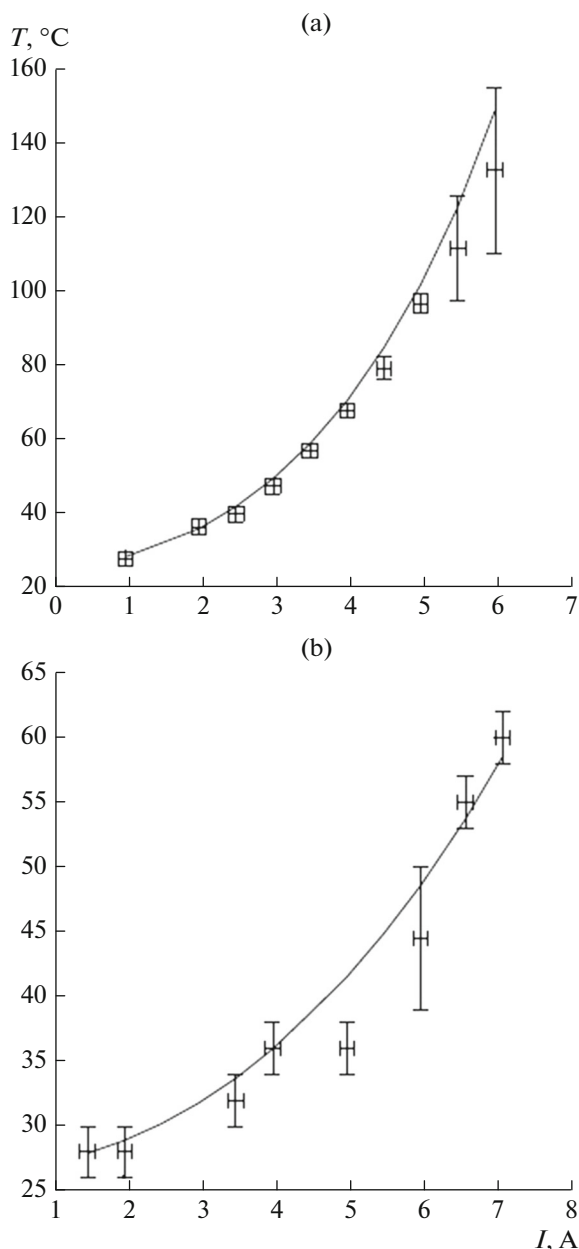


**Fig. 4.** Experimental and theoretical flowing current dependences of the temperature (a) at the bypass center and (b) near the interior angle of the conductor bent at a right angle.

achieve physical similarity with a geometrical one. In our opinion, this can be done mainly by changing the

heat-transfer coefficient; however, the engineering of this variant is beyond the scope of our study.

## REFERENCES

1. Lai, Y.-S. and Kao, C.-L., *Microelectron. Reliab.*, 2006, vol. 46, p. 1357.
2. Lai, Y.-S. and Kao, C.-L., *Microelectron. Reliab.*, 2006, vol. 46, p. 915.
3. Zhang, K. and Gong, L., *Arch. Elektrotech.*, 1993, vol. 76, p. 423.
4. Gerasimenko, T.N., Ivanov, V.I., Polyakov, P.A., and Popov, V.Yu., *J. Math. Sci.*, 2011, vol. 172, no. 6, p. 761.
5. Gerasimenko, T.N., Polyakov, P.A., and Frolov, I.E., *PIER Lett.*, 2014, vol. 47, p. 41.
6. Gerasimenko, T.N. and Polyakov, P.A., *Moscow Univ. Phys. Bull.*, 2012, vol. 67, p. 296.
7. Remsburg, R., *Thermal Design of Electronic Equipment*, Boca Raton: CRC Press, 2001.
8. Guenin, B.M., Marrs, R.C., and Molnar, R.J., *IEEE Trans. Compon., Packag., Manuf. Technol.*, 1995, vol. 18, p. 749.
9. Shaukatullah, H., Gaynes, M.A., and White, L.H., in *Proc. 4th Intersociety Conf. on Thermal Phenomena in Electronic Systems*, Washington, 1994, p. 237.
10. Grigor'ev, I.S. and Meilikhov, E.Z., *Fizicheskie velichiny: Spravochnik* (Physical Quantities: Handbook), Moscow: Energoatomizdat, 1991, p. 438.
11. Kikoin, I.K., *Tablitsy fizicheskikh velichin. Spravochnik* (Tables of Physical Quantities. Handbook), Moscow: Atomizdat, 1976, p. 304.
12. Buckingham, E., *Phys. Rev.*, 1914, vol. 4, p. 345.
13. Norrie, D.H. and de Vries, G., *Introduction to Finite Element Analysis*, Academic, 1978.
14. <https://www.cs.cmu.edu/~quake/triangle.html>.
15. Davis, T.A., *UMFPACK User Guide*, Gainesville: Univ. of Florida, 2011.

*Translated by E. Bondareva*